Breakup couplings in ^{6}He+^{4}He elastic scattering

K. Rusek
Department of Nuclear Reactions, The Andrzej Sołtan Institute for Nuclear Studies, Hoża 69, 00-681 Warsaw, Poland

K. W. Kemper
Physics Department, Florida State University, Tallahassee, Florida 32306-4350

(Received 11 October 1999; published 16 February 2000)

The similarity between ^{6}He+^{4}He and ^{6}Li+^{4}He elastic scattering data suggests that a previously performed coupled-discretized-continuum channels (CDCC) analysis of ^{6}Li+^{4}He might be applicable to recently published data for the elastic scattering of ^{6}He from ^{4}He at the three c.m. energies of 11.6, 15.9, and 60.4 MeV. A two-body cluster $\alpha+2n$ structure of ^{6}He was assumed and couplings to the first excited state of ^{6}He at the excitation energy of 1.8 MeV as well as to the states in the continuum were taken into account by means of the CDCC method. The calculations based on the previously performed CDCC analysis of polarized ^{6}Li+^{4}He scattering at a c.m. energy of 11.1 MeV provide a satisfactory description of the angular distributions of elastically scattered ^{6}He even at backward angles. This result suggests that the large angle scattering has a much smaller two-neutron transfer component than is commonly believed to be present.

PACS number(s): 24.10.Eq, 25.70.Bc

I. INTRODUCTION

The analysis of the elastic scattering of an exotic ^{6}He beam from a ^{4}He target measured recently at the center of mass (c.m.) energy of 60.4 MeV in Dubna [1] provided empirical evidence for a dineutron configuration in the neutron-rich ^{6}He nucleus. The angular distribution of elastically scattered ^{6}He could be reproduced at c.m. scattering angles up to 100° by an optical model (OM) calculation, while at more backward angles, the two-neutron exchange process dominated over simple potential scattering. The correct description of the back angle scattering data was achieved when a dineutron configuration for ^{6}He was assumed with the spectroscopic factor for the dineutron cluster, here denoted as $2n$, equal to unity.

The nucleus ^{6}He has much in common with the loosely bound nucleus ^{6}Li. Both nuclei are characterized by a large rms matter radius of 2.5–2.6 fm [2]. They do not have any bound excited states. The first excited state of ^{6}Li is a narrow resonance at the excitation energy of 0.712 MeV above the $^6\mathrm{Li}\rightarrow\alpha+d$ breakup threshold. The first excited state of ^{6}He is also a resonance at an excitation energy of 0.825 MeV above the $^6\mathrm{He}\rightarrow\alpha+2n$ breakup threshold [3]. The breakup thresholds for ^{6}Li and ^{6}He are at 1.474 MeV and 0.975 MeV, respectively. Because the main component of the ^{6}He ground state wave function corresponds to the cluster $\alpha+2n$ configuration, similar to the well-known $^6\mathrm{Li}=\alpha+d$ cluster structure, one may surmise that the scattering data of both nuclei on the same target and at the same c.m. energy should be similar.

Comparison of the recently published angular distribution of the differential cross section for ^{6}He+^{4}He elastic scattering at 11.6 MeV c.m. energy [4] with the ^{6}Li data measured at Florida State University at the very close c.m. energy of 11.1 MeV [5] shows that they exhibit great similarities. The values of the differential cross section for both scattering systems are of the same magnitude, and as can be seen in Fig. 1, the shapes of both angular distributions are also very similar. Since the sequential and direct breakup of ^{6}Li into an α particle plus a deuteron was found to play a very important role in ^{6}Li+^{4}He scattering [6], one can surmise that analogous effects can also be important for the ^{6}He+^{4}He system. Thus, a study similar to that for ^{6}Li+^{4}He would be of particular interest.

In this paper, we present the results of an analysis of existing ^{6}He+^{4}He elastic scattering data measured at the three c.m. energies of 11.6, 15.9, and 60.4 MeV [4,1]. The analysis is based on our experience with the ^{6}Li+^{4}He system, where the analyzing powers provided a large set of observables to test the CDCC method for this system. The goal of the present analysis is to determine the extent to which a simple two-body $\alpha+2n$ model of ^{6}He, analogous to the previously used $\alpha+d$ model of ^{6}Li, can reproduce the experimental cross sections when coupling to breakup channels is taken into account.

II. MODEL

A. Wave functions

The nucleus ^{6}He was assumed to have a two-body cluster $\alpha+2n$ structure with the spin of the $2n$ cluster set to $s=0$.

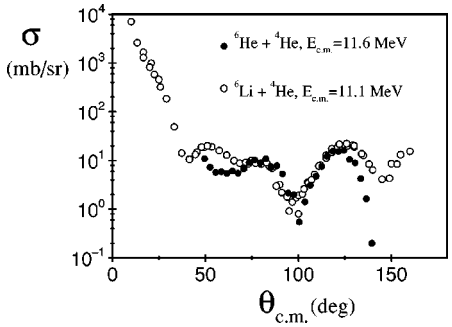

FIG. 1. Comparison of the angular distributions of the differential cross sections for ^{6}Li and ^{6}He elastically scattered from ^{4}He at similar c.m. energies. The experimental data are from Green *et al.* [5] and Raabe *et al.* [4].

The geometry of the Woods-Saxon potential between the clusters was taken to be the same as previously used for $^6\mathrm{Li}=\alpha+d$, with the radius equal to 1.9 fm and a diffuseness of 0.65 fm [7]. The wave function describing the relative motion of the two clusters in the ground state was calculated in the potential well with the depth varied to reproduce the binding energy of 0.975 MeV.

For the 2^+ resonance at excitation energy $E_x=1.80$ MeV, corresponding to the relative motion of the two clusters with orbital angular momentum $L=2$, the energy bin of 300 keV width was set at the mean energy of 0.825 MeV above the breakup threshold. The width of the bin roughly corresponds to the empirical value [8]. The wave function $\Psi(r)$ was calculated using the coupled-discretized-continuum-channels (CDCC) method. The cluster wave functions $\phi(r,k)$ in the bin, where $\hbar k$ is the momentum of the α-$2n$ relative motion, were averaged over the bin width Δk and normalized to unity according to [9,10]

$$\Psi(r)=\frac{1}{\sqrt{N\Delta k}}\int_{\Delta k}\phi(r,k)dk, \tag{1}$$

where N is the normalization factor and r is the α-$2n$ separation. The depth of the α-$2n$ potential was adjusted to give a resonance at the required excitation energy of 1.80 MeV. In the course of the analysis a test calculation was performed with a second $L=2$ resonance placed at an excitation energy of 3.3 MeV above the breakup threshold as suggested by Danilin *et al.* [8]. Its wave function was calculated in the same way, within the energy bin of 2.4 MeV width. The values of the excitation energies, bin widths, and potential depths found in the course of the calculations for the three discrete states of ^{6}He are listed in Table I.

The separations of the α-$2n$ clusters in the ^{6}He ground and 2^+ excited states can be characterized by the rms radii, calculated using the cluster wave functions. The obtained values are 4.92 fm and 6.78 fm, respectively. For comparison, the rms radius of the deuteron distribution in the ^{6}Li ground state was 4.06 fm and in the first excited state 4.19 fm [6]. Larger values for ^{6}He are due to the lower binding energy of the ground state and the larger width of the resonance.

The value of the reduced transition probability $B(E2;0^+\rightarrow 2^+)$, between the ground and 2^+ excited states, calculated using the cluster wave functions, is equal to $6.96e^2\,\mathrm{fm}^4$, which is larger than reported recently by Aumann *et al.* [11] $(3.2e^2\,\mathrm{fm}^4)$ or used in the model calculations by Görres *et al.* [12] $(2.85e^2\,\mathrm{fm}^4)$. However, as these values are model dependent, this difference is not significant.

TABLE I. Widths of the $L=2$ resonant bins and depths of the $\alpha+2n$ binding potential for the ground state and $L=2$ resonances (in MeV).

E_x	ΔE	V
0.000	0.000	69.363
1.800	0.300	80.531
4.275	2.400	69.330

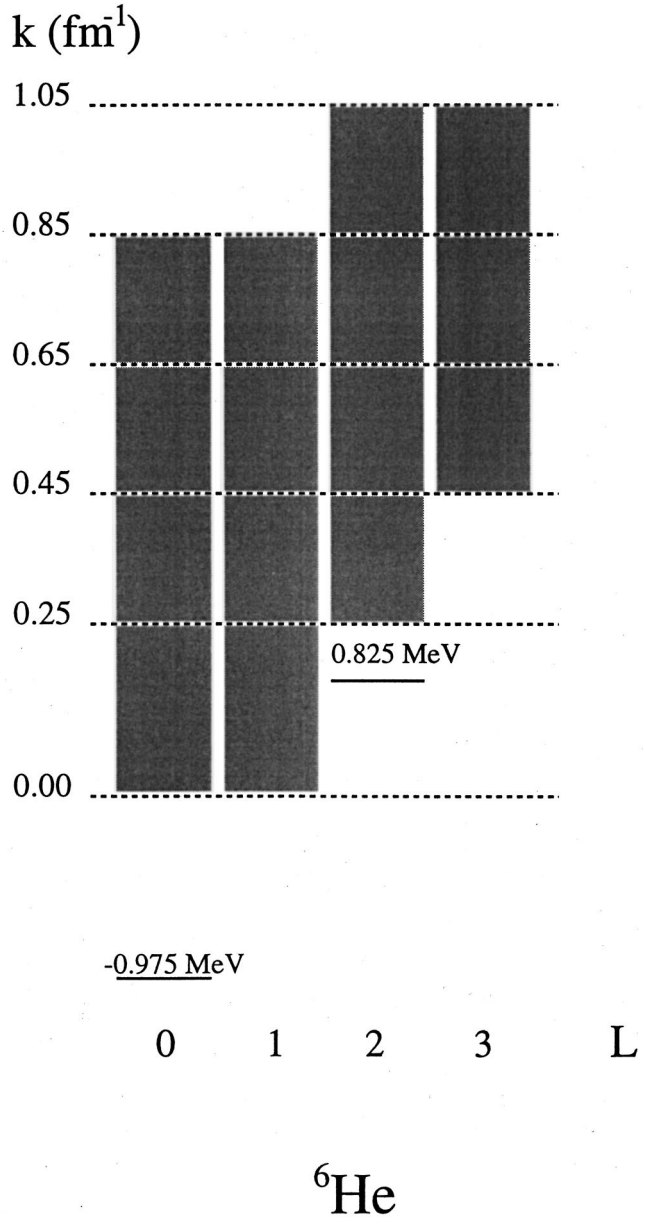

FIG. 2. Discretization of the ^{6}He continuum with respect to the momentum k of the $\alpha+2n$ relative motion used in the calculations for $E_{c.m.}=60.4$ MeV. For the two lower energies the range of the continuum states was appropriately limited.

Couplings to the continuum were realized by means of the CDCC method. The continuum above the breakup threshold was discretized into a series of momentum bins as shown in Fig. 2. For ^{6}He+^{4}He scattering at the c.m. energies of 11.6 and 15.9 MeV, the full momentum space was taken into account. At the highest c.m. energy of 60.4 MeV the model space was limited to the momentum of the α-$2n$ relative motion $\hbar k=1.05\hbar$ fm^{-1}, which corresponds to an excitation energy of about 18.3 MeV. The widths of the lowest bins just above the breakup threshold were set to $\Delta k=0.25$ fm^{-1} while the upper bins were of 0.20 fm^{-1} width. Those values were found to be sufficient to describe ^{6}Li

TABLE II. Parameters of the particle-^{4}He optical model potentials.

Particle	U_0 (MeV)	W (MeV)	X_0 (fm)
α	106.0	0.0	2.236
$2n$	64.1	2.5	2.236

scattering from ^{4}He, ^{26}Mg, ^{58}Ni, and ^{208}Pb [6,13–15]. The depth of the α-$2n$ potential for the continuum states was set to the value of 77.5 MeV, previously used for ^{6}Li scattering [6,13–15].

In the coupled-channels (CC) calculations each momentum bin was treated as an excited state of ^{6}He at an excitation energy equal to a mean energy $\langle E_x \rangle$ of the bin and spin equal to the relative momentum L between the α particle and $2n$ in the cluster system. The values of L were limited to $L=0,1,2,3$. The ^{6}He+^{4}He scattering wave functions were calculated at $\langle E_x \rangle$ and assumed to be energy independent within a particular bin. In a series of test calculations it was found that $L=2$, $0.0 \leqslant k \leqslant 0.25$ fm^{-1} as well as $L=3$, $0.0 \leqslant k \leqslant 0.45$ fm^{-1} bins have a negligible influence on the ^{6}He+^{4}He elastic scattering. Therefore those bins were omitted in the calculations in order to reduce the number of channels.

B. Interactions

All the central and coupling potentials used in the CC calculations, $V_{i \to f}(R)$, were derived from α-^{4}He and $2n$-^{4}He potentials $U_{\alpha,2n}$ by means of the single-folding method,

$$V_{i \to f}(R) = \left\langle \Psi_i(r) \left| U_{2n}\left(\left| \vec{R} + \frac{2}{3}\vec{r} \right| \right) + U_{\alpha}\left(\left| \vec{R} - \frac{1}{3}\vec{r} \right| \right) \right| \Psi_f(r) \right\rangle, \quad (2)$$

where R is the ^{6}He-^{4}He separation. The cluster-^{4}He input potentials were assumed to have a Gaussian shape [16],

$$U_i(X) = -U_{0,i} \exp\left[-\left(\frac{X}{X_0} \right)^2 \right], \quad (3)$$

where X is the separation between the cluster i and ^{4}He target nucleus. The α-^{4}He potential was assumed to be purely real. For ^{6}He+^{4}He scattering at 11.6 MeV c.m. energy this is justified by the large binding energy of the α particle. The parameters of the $2n$-^{4}He real potential were assumed to be the same as for d-^{4}He [16]. Moreover, a small imaginary part was added to this potential with a depth of $W=2.5$ MeV and the same geometry as for the real potential. The parameters of the input potentials to the single-folding calculations are listed in Table II.

In Fig. 3 the real part of the central ^{6}He+^{4}He potential resulting from the single-folding model calculation is compared to the empirical potential used by Ter-Akopian *et al.* [1] and to the potential derived from a realistic ^{6}He matter density by means of the double-folding model [17]. The single-folding potential at ^{6}He-^{4}He separations larger than 6 fm is very close to that used in the empirical analysis of ^{6}He+^{4}He elastic scattering at 60.4 MeV c.m. energy by Ter-Akopian *et al.* [1]. An OM calculation with this single-folding potential plus the imaginary part used by Ter-Akopian *et al.* [1] describes the exerimental data of the differential cross section at forward angles as well as the calculation presented in Ref. [1]. The potential derived by Baye *et al.* [17] is much less diffuse than the empirical potential and the potential used in this work.

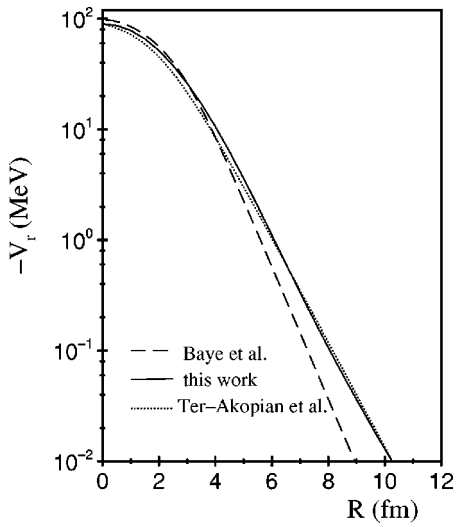

FIG. 3. Comparison of the real parts of the ^{6}He+^{4}He potential derived by means of the double-folding model by Baye *et al.* [17], that obtained in this work from single-folding calculations, and the empirical potential found from a fit to the experimental data by Ter-Akopian *et al.* [1].

III. RESULTS OF THE CALCULATIONS

A. Inelastic excitations

The CDCC calculations were performed using version FRXP-15 of the coupled-reaction channels code FRESCO [9]. The coupled equations were integrated out to 30 fm and 100 partial waves were used. All the parameters of the model were kept fixed for the three incident energies of ^{6}He beam. In the course of the analysis more attention was payed to the 60.4 MeV data set since at the low c.m. energy the ^{6}He excitation curve could exhibit a resonance behavior. The results of the analysis are compared to the experimental data in Fig. 4.

The calculations reproduce the values and the shape of the angular distribution of the differential cross section for $E_{c.m.}=11.6$ MeV. At the highest energy of 60.4 MeV the calculation reproduces the forward angle scattering data including an oscillation at about 25°. At backward scattering angles the calculation predicts a rise of the differential cross section which is observed experimentally. The two low energy data sets do not exhibit an energy dependence and the angular distribution measured at 15.9 MeV is almost identical with that obtained at 11.6 MeV. This insensitivity to the incoming energy is not confirmed by the calculations and the calculated angular distribution at 15.9 MeV is shifted back-

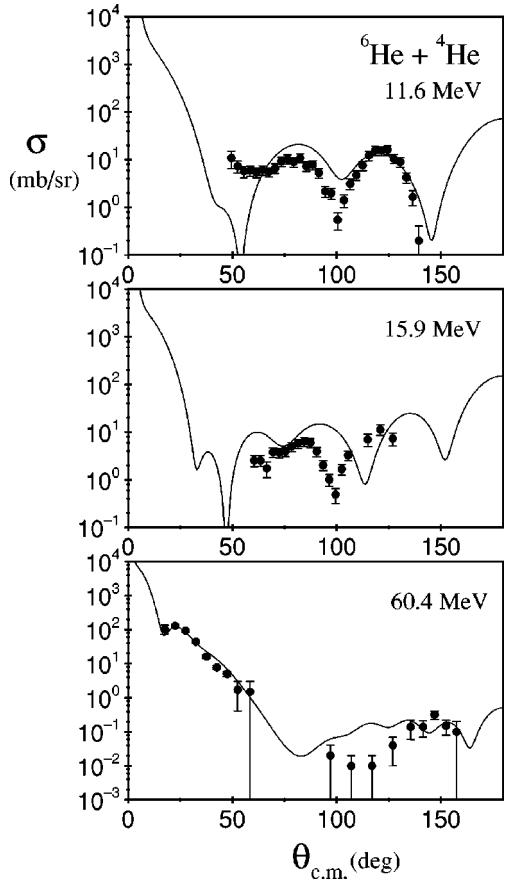

FIG. 4. Results of the CDCC calculations for ^{6}He+^{4}He elastic scattering at three c.m. energies. The data sets are from Refs. [1,4].

wards by about 15° in comparison with the data. For ^{6}Li scattering at 11.6 and 15.0 MeV, the expected shift to smaller angles at higher energy is observed [5], suggesting that resonance contributions are present at the higher ^{6}He energy.

Coupling to the breakup channels is found in the course of the calculations to affect considerably the process of elastic scattering at all three energies. In Fig. 5 the effects generated by the couplings to the different breakup channels are shown for the c.m. energy of 60.4 MeV. The OM calculation over-

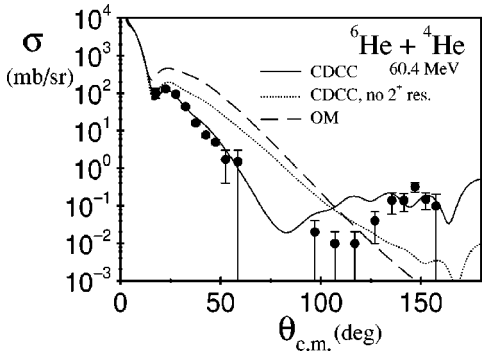

FIG. 5. The effects of sequential and direct breakup of the projectile on ^{6}He+^{4}He elastic scattering at the c.m. energy of 60.4 MeV. The data set is from Ref. [1]. See text for details.

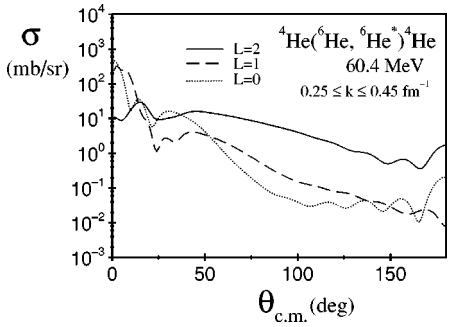

FIG. 6. Calculated angular distribution of the differential cross section for the ^{6}He+^{4}He→(^{6}He*=$\alpha+2n$)+^{4}He inelastic scattering at the c.m. energy of 60.4 MeV corresponding to the $\alpha+2n$ momentum bin ranging from $0.25\hbar$ to $0.45\hbar$ fm^{-1}. The curves show contributions due to the different relative orbital momentum L of the two clusters.

estimates the measured values of the differential cross section up to 120° as shown by the dashed curve. Inclusion of the coupling to the resonance at $E_x=1.80$ MeV reduces the calculated values of the cross section at forward angles and enlarges them at more backward angles. Couplings to the nonresonant states further improve the description (solid curve).

CDCC calculations predict a rise of the ^{6}He+^{4}He elastic scattering differential cross section at backward angles. This effect was seen in the experiment by Ter-Akopian *et al.* [1] and interpreted as a contribution from the two-neutron exchange process, not distinguished experimentally from elastic scattering. In the present calculations this rise emerges naturally from coupling to the breakup channels. Coupling to the 2^+ resonance plays an especially important role as illustrated in Fig. 5. The calculations without this resonance, shown by the dotted curve, do not describe the experimental data.

This sensitivity to the $L=2$ resonance was further exploited to test whether the elastic scattering data probe the structure of the $L=2$ continuum. Predictions made by Danilin *et al.* [8], based on a three-body $\alpha+n+n$ cluster structure of ^{6}He, suggested the existence of a second 2^+ quadrupole resonance at an excitation energy of 3.3 MeV above the breakup threshold. Present CDCC calculations with this resonance included and represented by the wave function generated as described in the previous section produced a worse description of the experimental data at all three ^{6}He incident energies.

In Fig. 6, the angular distributions of the differential cross section for the direct $^6\mathrm{He}\rightarrow\alpha+2n$ breakup corresponding to the excitation energy ranging from about 2.0 MeV up to 4.0 MeV are shown. At backward scattering angles the breakup is dominated by $L=2$ cluster states and coupling to these breakup channels is mainly responsible for the rise in the elastic scattering cross section at backward angles.

The total scattering amplitude can be decomposed into components of near-side and far-side scattering. Such decomposition is used for exploring the role of coupling effects in the scattering [18]. The ^{6}He+^{4}He potential scattering at $E_{c.m.}=60.4$ MeV is dominated by the far-side component.

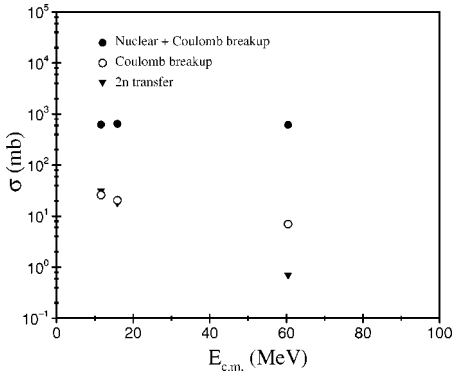

FIG. 7. Energy dependence of the calculated ^{6}He total breakup cross section (solid circles), its component due to the Coulomb interactions (open circles) and the cross section for the dineutron transfer reaction.

As a result of this component, the results of the OM calculation overestimate the experimental data. Couplings to the breakup channels reduce the far-side component while the near-side component remains almost unchanged. The domination of the far-side scattering is not so evident at low energy but also, there, couplings to the breakup channels reduce mainly the far-side scattering. This effect can be simulated by a reduction of the central attractive (real) nuclear potential. Thus, couplings to the sequential and direct breakup channels produce a polarization potential of a repulsive nature, analogous to that seen previously for ^{6}Li scattering [18].

The total breakup cross section was found in the course of the calculations to be almost independent of scattering energy as plotted in Fig. 7. At 60.4 MeV the value of the calculated total breakup cross section was equal to 606 mb while at 11.6 MeV it was slightly larger, 637 mb. This similarity is a result of the fact that the description of the three data sets could be achieved with the fixed depth of the imaginary part of the $2n$-^{4}He potential used as an input to the single-folding calculations. The contribution to the total breakup cross section due to the Coulomb interactions is found to be very small. The whole process is mainly driven by nuclear forces. With increasing incident energy the Coulomb contribution becomes smaller.

As shown in Fig. 8, the main contribution to the total breakup cross section comes from the states corresponding to the ^{4}He-$2n$ relative motion with orbital angular momentum $L=2$. However, just above the breakup threshold, $L=2$ states contribute negligibly to the total breakup spectrum, since the spectrum is dominated by $L=0$ and $L=1$ states. It is interesting to note that the angular distributions of the differential cross section for the two contributions are very similar which makes it difficult to distinguish between them. Breakup states with $L=3$ start to be important at excitation energies higher than 4 MeV.

B. Dineutron transfer

The process of exchanging a dineutron between the projectile and the target nucleus is experimentally indistinguishable from elastic scattering and therefore has to be taken into account in the data analysis. In the present analysis the transfer of the dineutron from the ^{6}He$_{g.s.}$ is taken into account by means of the coupled-reaction-channels (CRC) method and after correction for the scattering angle coherently added to the elastic scattering amplitudes.

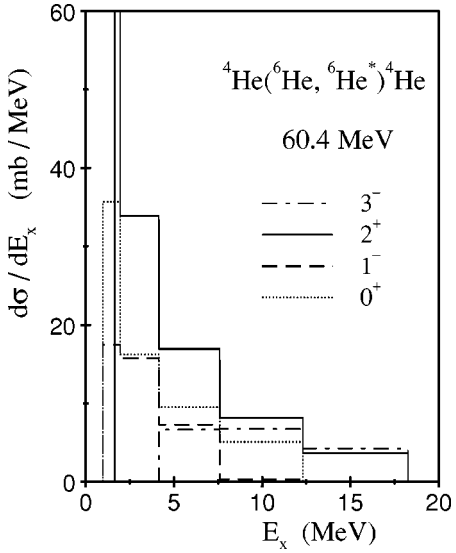

FIG. 8. Calculated spectrum for ^{6}He+^{4}He$\rightarrow$(^{6}He*$=\alpha+2n$) +^{4}He inelastic scattering at the c.m. energy of 60.4 MeV. Here E_x denotes the excitation energy of the ^{6}He$=\alpha+2n$ cluster system. The curves show contributions from the $\alpha+2n$ breakup states corresponding to the relative motion of the two clusters with orbital angular momentum $L=0,1,2,3$.

The total cross section for this process is the largest at the c.m. energy of 11.6 MeV and decreases with increasing incident energy more rapidly than that for Coulomb excitation (see Fig. 6). The transfer of the dineutron modifies the results of the CDCC calculations for the angular distributions of the elastic scattering differential cross section at angles other than the forward ones. An example is shown in Fig. 9. The results of calculations with effects of ^{6}He breakup included by means of the CDCC method are shown by the dashed curve. The dotted curve presents calculated angular distribution of the dineutron transfer process, corrected for the scattering angle. The results of the final CRC calculations, taking into account the effects of breakup and dineutron transfer,

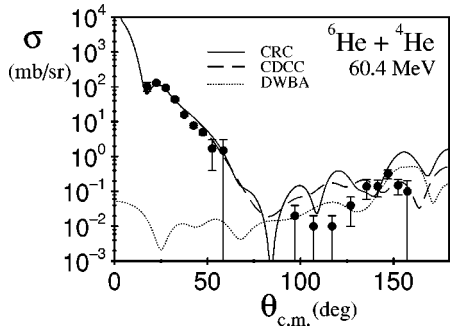

FIG. 9. The effect of the dineutron transfer reaction on the calculated differential cross section for ^{6}He+^{4}He elastic scattering at the c.m. energy of 60.4 MeV. The data set is from Ref. [1].

are plotted by the solid curve. Inclusion of the transfer generates a more oscillatory shape of the calculated angular distribution, with a deep minimum at about 80° c.m. in the scattering angle. For the 15.9 MeV data set the inclusion of the transfer has a much weaker effect, while for the lowest energy of 11.6 MeV it deteriorates the description of the data obtained by the CDCC calculation.

IV. CONCLUSIONS

The present analysis of ^{6}He+^{4}He elastic scattering data at the three c.m. energies of 11.6, 15.9, and 60.4 MeV by means of CDCC calculations supports the suggestion [1,19] that the experimental data can be described in terms of a simple two-body model of ^{6}He. In this model, ^{6}He was assumed to consist of an α core and a dineutron cluster bound by a potential analogous to that used previously for $\alpha+d$ clusters forming the nucleus ^{6}Li.

At higher energy, the CDCC calculations reproduced the forward angle scattering data including an oscillation at about 25°. For these angles, the role of breakup is similar to that found for other loosely bound nuclei like ^{6,7}Li or ^{9}Be: coupling to the breakup channels reduces the far-side scattering amplitude. This reduction can be simulated by a repulsive polarization potential. At more backward scattering angles, complicated coherent effects arise mainly from coupling to the $L=2$ breakup states so that the elastic scattering cross section is not reduced but enhanced.

The role of the dineutron transfer was investigated by means of the CRC method. Inclusion of the transfer influences the angular distribution of the differential cross section at backward scattering angles. The contributions of the transfer and ^{6}He breakup process are found to be of equal importance.

The present analysis is not able to answer the often raised question as to whether ^{6}He is a halo nucleus. The results obtained in the present work show that the scattering of ^{6}He can be treated in a two-body cluster model as is the scattering of ^{6}Li. The amount of available experimental data on ^{6}He scattering is at present very limited but new possibilities to perform experiments with ^{6}He beams will open in the near future. The results obtained in the present work show the need to perform scattering experiments with exotic ^{6}He beams on targets and at energies where ^{6}Li scattering data are already available so that the comparison between ^{6}He and ^{6}Li scattering may shed light on the details of the structure of ^{6}He.

ACKNOWLEDGMENTS

The authors thank Dr. Andreas Piechaczek for supplying the lower energy ^{6}He+^{4}He scattering data in tabular form, and for several very helpful discussions. This work was supported in part by the State Committee for Scientific Research (KBN) of Poland, the U.S. National Science Foundation, and NATO.

[1] G. M. Ter-Akopian, A. M. Rodin, A. S. Fomichev, S. I. Sidorchuk, S. V. Stepantsov, R. Wolski, M. L. Chelnokov, V. A. Gorshkov, A. Yu. Lavrentev, V. I. Zagrebaev, and Yu. Ts. Oganessian, Phys. Lett. B **426**, 251 (1998).

[2] I. Tanihata, T. Kobayashi, O. Yamakawa, T. Shimoura, K. Ekuni, K. Sugimoto, N. Takahashi, T. Shimoda, and H. Sato, Phys. Lett. B **206**, 592 (1988).

[3] F. Ajzenberg-Selove, Nucl. Phys. **A490**, 1 (1988).

[4] R. Raabe, A. Andreev, D. Baye, W. Bradfield-Smith, T. Davinson, M. Gaelens, W. Galster, M. Huyse, J. McKenzie, A. Ninane, A. Piechaczek, A. C. Shotter, G. Vancraeynest, P. Van Duppen, and A. Wöhr, Phys. Lett. B **458**, 1 (1999).

[5] P. V. Green, K. W. Kemper, P. L. Kerr, K. Mohajeri, E. G. Myers, D. Robson, K. Rusek, and I. J. Thompson, Phys. Rev. C **53**, 2862 (1996).

[6] K. Rusek, P. V. Green, P. L. Kerr, and K. W. Kemper, Phys. Rev. C **56**, 1895 (1997).

[7] K.-I. Kubo and M. Hirata, Nucl. Phys. **A187**, 186 (1972).

[8] B. V. Danilin, T. Rogde, S. N. Ershov, H. Heiberg-Andersen, J. S. Vaagen, I. J. Thompson, and M. V. Zhukov, Phys. Rev. C **55**, R577 (1997).

[9] I. J. Thompson, Comput. Phys. Rep. **7**, 167 (1988).

[10] J. E. Bowsher, T. B. Clegg, H. J. Karwowski, E. J. Ludwig, W. J. Thompson, and J. A. Tostevin, Phys. Rev. C **45**, 2824 (1992).

[11] T. Aumann, D. Aleksandrov, L. Axelsson, T. Baumann, M. J. Borge, L. V. Chulkov, J. Cub, W. Dostal, B. Eberlein, Th. W. Elze, H. Emling, H. Geissel, V. Z. Goldberg, M. Glovkov, A. Grünschloss, M. Hellström, K. Hencken, J. Holeczek, R. Holzmann, B. Jonson, A. A. Korshenninikov, J. V. Kratz, G. Kraus, R. Kulessa, Y. Leifels, A. Leistenschneider, T. Leth, I. Mukha, G. Münzenberg, F. Nickel, T. Nilsson, G. Nyman, B. Petersen, M. Pfüzner, A. Richter, K. Riisager, C. Scheidenberger, G. Schrieder, W. Schwab, H. Simon, M. H. Smedberg, M. Steiner, J. Stroth, A. Surowiec, T. Suzuki, O. Tengblad, and M. V. Zhukov, Phys. Rev. C **59**, 1252 (1999).

[12] J. Görres, H. Herndl, I. J. Thompson, and M. Wiescher, Phys. Rev. C **52**, 2231 (1995).

[13] K. Rusek, N. M. Clarke, and R. P. Ward, Phys. Rev. C **50**, 2010 (1994).

[14] K. Rusek, N. M. Clarke, G. Tungate, and R. P. Ward, Phys. Rev. C **52**, 2614 (1995).

[15] N. Keeley and K. Rusek, Phys. Lett. B **427**, 1 (1998).

[16] H. Nishioka, J. A. Tostevin, R. C. Johnson, and K. I. Kubo, Nucl. Phys. **A415**, 230 (1984).

[17] D. Baye, L. Desorgher, D. Guillain, and D. Herschkowitz, Phys. Rev. C **54**, 2563 (1996).

[18] Y. Sakuragi, Phys. Rev. C **35**, 2161 (1987).

[19] Yu. Ts. Oganessian, V. I. Zagrebaev, and J. S. Vaagen, Phys. Rev. Lett. **82**, 4996 (1999).